4.4a ENERGY SIMILARITY – A NEW TUBRULENCE CLOSURE MODEL FOR STABLE BOUNDARY LAYERS

Thorsten Mauritsen[1], Gunilla Svensson, Department of Meteorology, Stockholm University, Leif Enger and Sergej Zilitinkevich, Department of Earth Sciences, Meteorology, Uppsala University, Branko Grisogono, Department of Geophysics, Faculty of Science, Zagreb.

1 INTRODUCTION

The problem of scaling and modelling of the stably stratified atmospheric boundary layer is yet unresolved (Mahrt, 1999). Though, at the same time the stable regime is important in practical applications, such as dispersion of tracers, numerical weather prediction and climate modelling (eg. Viterbo et al., 1999).

Here we propose a new approach for scaling stably stratified turbulence. Here the fluxes of momentum and heat are directly related to the level of turbulent kinetic energy and temperature variance, through the energy similarity relations. In these relations the non-dimensional momentum and heat fluxes are assumed to be functions of the local gradient Richardson number only.

Measurements of the non-dimensional fluxes show reasonable agreement with recent theoretical results presented by Sukoriansky and Galperin (2004). Further, it is noted that these measures are void of self-correlation, which is otherwise common in stably stratified turbulence scaling (Mahrt and Vickers, 2003). This scaling is the base of a new closure implemented in a boundary-layer model. This model gives results that are in good agreement with large eddy simulations (LES) in a weakly stable case (Beare et al., 2004).

2 ENERGY-SIMILARITY SCALING

We concider stably stratified turbulent shear flows. These flows can be decomposed into mean-flow wind, $\mathbf{U} = (U, V)$, potential temperature, Θ, and the deviations from the means, $u, v, w$and θ, by the Reynolds averaging technique.

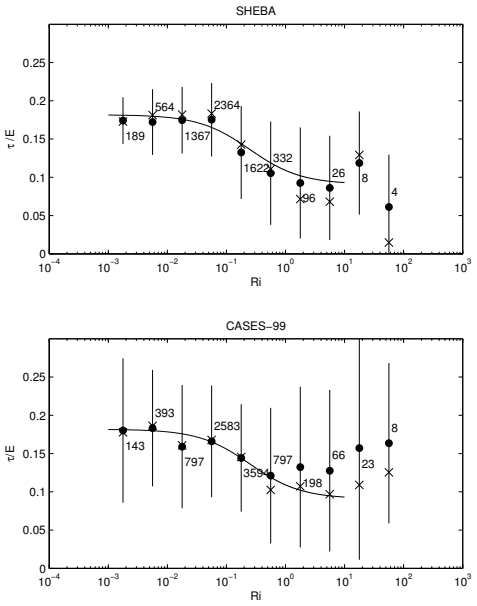

Figure 1: The non-dimensional momentum flux as a function of the local gradient Richardson number for two measurement campaigns. The dots are binned mean values, crosses are medians and the vertical bars show the standard deviations.

Of special interest is the vertical fluxes of momentum and heat, given by the ensemble average covariations, $\overline{uw}, \overline{vw}$ and $\overline{w\theta}$. We may relate these fluxes to the variance of the turbulent quantities, to obtain the non-dimensional fluxes:

$$\frac{|\tau|}{E} = f_\tau, \quad \frac{\overline{w\theta}}{\sqrt{E_\theta E}} = f_\theta, \tag{1}$$

where τ is the stress vector, $E \equiv 0.5(\overline{u^2} + \overline{v^2} + \overline{w^2})$ is the turbulent kinetic energy, $E_\theta \equiv 0.5(\overline{\theta^2})$ and f_τ and f_θ are unknown functions.

[1]Corresponding author: Department of Meteorology, Stockholm University, S-106 91 Stockholm, Sweden, email: thorsten@misu.su.se

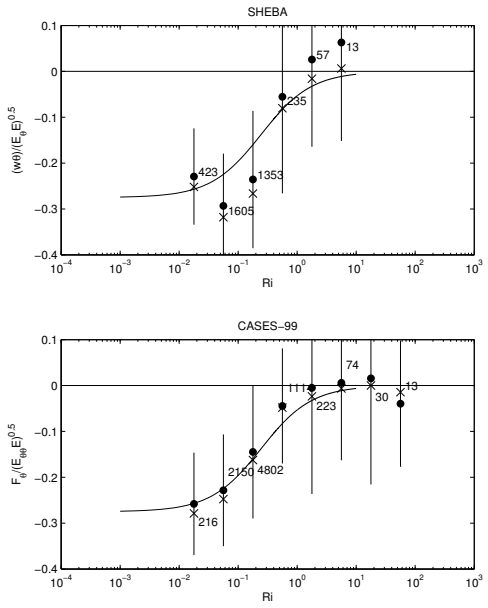

Figure 2: The non-dimensional heat flux as a function of Richardson number. Otherwise as Figure 1.

In stably stratified shear flows the turbulent whirls become anisotropic when the stratification dominates over the shear. As a consequence the mean flow gradient Richardson number:

$$Ri \equiv \frac{N^2}{S^2},$$

increases for increasing stability. At the same time gravity waves may become excited in stratified flows. The complex interaction between gravity waves and turbulence causes, among other things, the fluxes of momentum and heat to behave differently at at strong stability, since waves transport momentum efficiently but very little heat.

In Figures 1 and 2 we plot the non-dimensional fluxes obtained from mast-mounted instruments during the SHEBA and CASES-99 campaigns. Ri is calculated as centered differences from either sonics or wind-vanes/thermocouples, respectively. In SHEBA sonic anemometers, and in CASES-99 hot-film anemoters were used for measuring temperature variations. The former year-long dataset contains hourly means, while the latter one-month dataset is given in 5-minute averages. Cases with countergradient momentum fluxes are ignored, as they are likely to be influnced by non-local gravity waves. Further, it is required that $N > 0.02s^{-1}$ in Figure 2, in order to avoid non-local convective cases.

We note how the non-dimensional fluxes decreases for increasing Ri. However beyond $Ri \approx 0.1$ the non-dimensional heat flux decreases rapidly towards zero, while for momentum the flux seems to level off at about half of the near neutral value. Sukoriansky and Galperin (2004) use renormalization group theory to calculate the ratio of the turbulent viscosity and conductivity in stratified shear flows to their neutral limits. It can be shown that these ratios are the same as the non-dimensional fluxes multiplied by an empirical constant (Mauritsen et al., 2004). We approximated functions to their results:

$$f_E = 0.18\left(\frac{0.5}{1+4Ri}+0.5\right), \quad (2)$$

$$f_\theta = 0.27\left(\frac{1}{1+3Ri}\right), \quad (3)$$

and plotted them in the figures. For $Ri < 1$ there is good agreement between and observations, and even for larger Ri there is reasonable agreement.

Scaling of the non-dimensional fluxes using the gradient Richardson number is void of self-correlation, described in Mahrt and Vickers (2003). This means that no variable is used on both axis. In fact Ri contains only mean flow quantities, while the non-dimensional fluxes consist of variances and covariances of deviation quantities.

3 MODEL FRAMEWORK

Prognostic equations for the mean state wind and the mean potential temperature of the atmospheric turbulent boundary layer in

their Reynolds averaged form are:

$$-\frac{\partial \overline{uw}}{\partial z} - f(V_g - V) = \frac{DU}{Dt}, \quad (4)$$

$$-\frac{\partial \overline{vw}}{\partial z} + f(U_g - U) = \frac{DV}{Dt}, \quad (5)$$

$$-\frac{\partial}{\partial z} = \frac{D\Theta}{Dt}, \quad (6)$$

where f is the Coriolis parameter, primed variables are the excursions from their mean state value, an overline is the ensemble average and D/Dt denotes the total derivative. $\mathbf{U_g} = (U_g, V_g)$ is the background geostrophic wind vector.

In addition to the mean variables, among the equations for the second order moments, we keep two equation; equations for the turbulent kinetic energy and the potential temperature variance:

$$\tau \cdot \frac{\partial \mathbf{U}}{\partial z} + \frac{g}{\Theta}\overline{\theta w} - \epsilon = \frac{\partial F_E}{\partial z} + \frac{DE}{Dt}, \quad (7)$$

$$-\overline{\theta w}\frac{\partial \Theta}{\partial z} - \phi = \frac{\partial F_\theta}{\partial z} + \frac{DE_\theta}{Dt}, \quad (8)$$

ϵ and ϕ are the dissipation rates, and F_E and F_θ are the third-order vertical fluxes of turbulent kinetic energy and potential temperature variance, respectively.

In order to close the equation system we use equations (2) and assume that the dissipation rates are well described by the Kolmogorov-Heisenberg relations:

$$\epsilon = 0.08\frac{E^{3/2}}{l_\epsilon}, \ \phi = 0.13\frac{E_\theta\sqrt{E}}{l_\epsilon}, \quad (9)$$

where l_ϵ is the dissipation length scale, chosen for simplicity to be:

$$\frac{1}{l_\epsilon} = \frac{1}{0.4z} + \frac{N}{0.22\sqrt{E}}. \quad (10)$$

The closure constants in equations (9) and (10) where derived in Mauritsen et al. (2004)

4 RESULTS

A weakly stable case was presented by Kosovic and Curry (2000). Geostrophic winds were 8 m s^{-1} and the surface cooling rate -0.25 K h^{-1}. The case was chosen as a first intercomparison case in the GEWEX Atmospheric Boundary Layer Study (GABLS, Holtslag et al., 2003, Beare et al., 2004 and Cuxart et al. 2004).

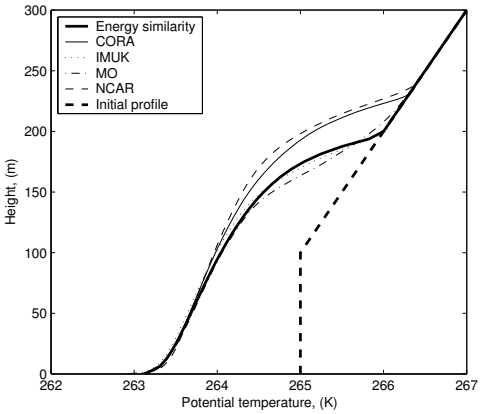

Figure 3: Potential temperature profiles after 9 hours of the GABLS case. Thick lines are the initial and final profile for the energy similarity closure model, while thin lines are 2 m resolution LES.

In Figures 3 and 4 we show the potential temperature profile and timeseries of the boundary layer height, surface heat flux and friction velocity, and the Monin-Obukhov length. It is generally seen that the energy similarity closure model is able to reproduce the results of the 2 m resolution LES, with the choice of dissipation length (10). It is however still a matter of debate, whether the LES are reproducing a realistic ensemble mean boundary layer (Cuxart et al., 2004).

References

Beare, R. J. et al., 2004. An intercomparison of large-eddy simulations of the stable boundary layer. *16th Symposium on Boundary Layers and Turbulence, proceeding 4.1.*

Cuxart, J. et al., 2004. Single-column intercomparison for a stably stratified atmo-

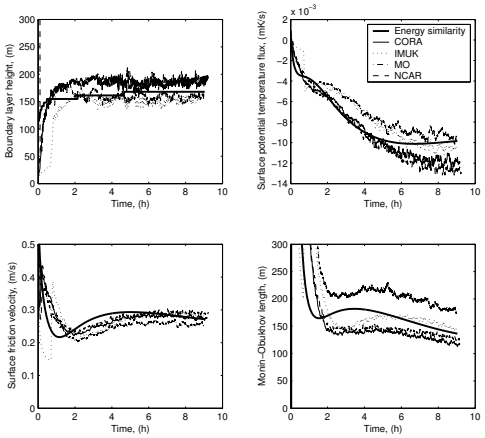

Figure 4: Timeseries of various properties. etherwise as in Figure 3.

spheric boundary layer. *To be submitted to Bound.-Layer Meteorol.*

Holtslag, A. A. M., R. J. Beare and J. Cuxart Rodamilans, 2003. GABLS workshop on stable boundary layers. *GEWEX News*, November, 11–13.

Kosovic, B., and J. A. Curry, 2000. A large eddy simulation study of a quasi-steady, stably stratified atmospheric boundary layer. *J. Atmos. Sci.* **57**, 1052–1068.

Mahrt, L., 1999. Stratified atmospheric boundary layers. *Bound.-Layer Meteorol.* **90**, 375–396.

Mahrt, L., and D. Vickers, 2003. Formulation of Turbulent Fluxes in the Stable Boundary Layer. *J. Atmos. Sci.* **60**, 2538–2548.

Mauritsen, T., S. S. Zilitinkevich, L. Enger, G. Svensson and B. Grisogono, 2004. An energy similarity closure model for the stable atmospheric boundary layer. *Manuscript.*

Nieuwstadt, F. T. M., 1984. Turbulent structure of the stable, nocturnal boundary layer. *J. Atmos. Sci.* **41**, 2202–2216.

Sukoriansky, S., and B. Galperin, 2004. A spectral closure model for turbulent flows with stable stratification. *Marine Turbulence - Theories, Observations and Models.* H. Baumert, J. Simpson, J. Sundermann, Eds., Cambridge University Press, in press.

Viterbo, P., Beljaars, A. C. M., Mahfouf, J.-F. and Teixeira, J., 1999. The representation of soil moisture freezing and its impact on the stable boundary layer. *Quart. J. Roy. Meteorol. Soc.*, **125**, 2401–2426.